Life history strategies explain bacterial activity in the soil carbon cycle

Samuel E. Barnett[a*], Nicholas D. Youngblut[a,b*], Chantal N. Koechli[a,c], and Daniel H. Buckley[a]

a. School of Integrative Plant Science, Cornell University, Ithaca, NY, USA
b. Department of Microbiome Science, Max Planck Institute for Developmental Biology, Tübingen, Germany
c. Department of Biological Sciences, University of the Sciences, Philadelphia, NY, USA
* Co-first authors

Corresponding author: Daniel H. Buckley
dbuckley@cornell.edu

ORCIDs: 0000-0002-0096-0605, 0000-0002-7424-5276, NA, 0000-0003-1654-2907

Keywords: DNA-SIP, bacterial, soil, carbon cycling, ecology

Author contributions: NDY and DHB conceived of the study, NDY and CNK conducted the experiment and collected all the data, NDY and DHB analyzed the data, NDY, SEB, and DHB wrote the manuscript. All authors were involved in editing and reviewing manuscript.

Competing interests: The authors declare no competing interests.

Abstract

Soil microorganisms determine the fate of soil organic matter (SOM), and their activities comprise a major component of the global carbon (C) cycle. We sought to comprehend the physiological and ecological mechanisms underpinning microbial contributions to SOM dynamics by examining the activities of individual microorganisms within a complex soil system. We determined bacterial activity by using a multi-substrate DNA-stable isotope probing experiment to track C assimilation dynamics across thousands of bacteria within an agricultural soil. In this way, we identified 1,286 bacterial taxa assimilating C from SOM. Substrate bioavailability explained significant variation in mineralization rates and microbial assimilation dynamics. We show that, while patterns of C assimilation exhibited little phylogenetic conservation above the species level, these patterns defined functional clusters whose properties exemplified broad differences in life history strategy, particularly along the copiotroph-oligotroph continuum. We also show that these functional clusters explain soil community response to fresh litter, and patterns of microbial biogeography at continental and global scales. Our results add to the growing body of knowledge indicating that life history theory provides a useful framework for understanding microbial contributions to terrestrial C-cycling.

Introduction

Soil organic matter (SOM) represents the largest terrestrial pool of organic carbon (C) on Earth [1], and SOM dynamics have major impacts on the global C-cycle. SOM is sensitive to land management [2–4] and climate change [5], and SOM pools influence soil health [6, 7], agricultural productivity [8], and climate stability [6, 9]. However, the mechanisms that promote SOM persistence and loss remain uncertain and this introduces variability into global C-cycle models [10–13]. Microorganisms are dominant drivers of SOM decomposition, stabilization, and mineralization [14], and C-cycle models increasingly seek to incorporate microbial traits to improve predictions of SOM dynamics [15, 16]. For example, microbially explicit C-cycle models, such as MEND [17], MIMICS [18], and CORPSE [19], improve prediction of C-cycle dynamics when compared to models that ignore microbial processing [20].

Soil microbes play a critical role in governing global C flux, but the microbial mechanisms that determine SOM dynamics remain poorly characterized [13]. Microbial contributions to soil C-cycling are typically determined in the aggregate (*e.g.,* soil respiration) without providing mechanistic insight into processes of individual microbes. Determining the functional abilities of individual microbes typically requires laboratory cultivation, but most soil microbes remain uncultivated and poorly characterized [21–23]. In the absence of cultivation, the functions of uncultivated microbes are often inferred by assuming phylogenetic conservation with cultivated representatives [24–26]. However, phylogenetic conservation varies dramatically among microbial traits and functionalities [27], and many soil microbes lack closely related cultivated isolates [28]. Alternatively, microbial functions can be inferred through metagenomic analyses, which indicate the frequency of specific gene families and metabolic pathways in the environment [29, 30].

Inferences based on phylogenetic conservatism and metagenomic analyses predict 'potential function', and not whether a function is realized *in situ*. Microbe-microbe and microbe-environment interactions alter patterns of gene expression, activity, and growth, and so potential function tells us little of the 'realized functions' manifesting in soil at any particular place and time. The realized functions of microbes *in situ* depend on a complex pattern of biotic and abiotic interactions, and the functions realized at any given place and time might correlate only weakly with the functional potential of the community inferred from metagenomic analyses [31, 32].

An alternative approach to predicting microbial activity in the C-cycle is to focus on microbial life history strategies [33]. Life history strategies describe combinations of traits that govern energy allocation to growth, resource acquisition, and survival [34, 35]. Since stabilized SOM is largely composed of the products of microbial anabolic metabolism, microbial growth dynamics are likely a major determinant of C fate in soil [14]. Life history theory proposes that fitness optimization imposes tradeoffs on energy allocation [36, 37]. For example, growth rate and substrate use efficiency correlate negatively in heterotrophic microbes [38]. This growth versus efficiency tradeoff is foundational to the copiotrophy/oligotrophy hypothesis used to explain microbial ecological dynamics [39]. Copiotrophs are characterized as microbes that maximize fitness when nutrient flux across the cell membrane is high, having high maximum growth rate but low carbon use efficiency. Oligotrophs are characterized as microbes that maximize fitness when nutrient flux across the membrane is low, having low maximum growth rate and high carbon use efficiency [40–42]. Growth parameters associated with life history strategies (*e.g.,* growth rate and carbon use efficiency) can be readily modeled [18] and are of high relevance to the C-cycle [43, 44]. While much focus in the literature emphasizes

84 copiotrophs and oligotrophs, many different tradeoffs impact microbial resource allocation to
85 growth and survival and these tradeoffs likely define diverse microbial life history strategies in
86 soil. However, direct observation of realized microbial activities as they occur *in situ* is
87 necessary to inform and refine our understanding of microbial life history strategies in soil.
88 DNA-stable isotope probing (DNA-SIP) can assess the realized function of microbes
89 within complex habitats [45] by identifying specific taxa that have incorporated isotopes from a
90 labeled substrate into their biomass [45]. DNA-SIP can track the assimilation of C from multiple
91 substrates into thousands of microbial taxa in soil [46–48] with high specificity and sensitivity
92 [48]. We used multiple-window high-resolution DNA-SIP (MW-HR-SIP) to track bacterial
93 utilization of C derived from nine distinct substrates that vary in bioavailability and are common
94 in soils (Fig. 1). We defined bioavailability on the basis of solubility and hydrophobicity, which
95 predicts sorption to particulate organic matter [49] and substrate availability for transport across
96 the cell membrane. The substrates include cellulose (a component of plant cell walls), glucose
97 and xylose (monomers of cellulose and hemicellulose respectively), vanillin (a phenolic acid
98 derived from lignin), glycerol and palmitic acid (components of plant lipids), an amino acid
99 mixture (monomers of protein), and lactate and oxalate (major fermentation products from soil
100 bacteria and fungi). Our multi-substrate design, where only the identity of the ^{13}C-substrate was
101 varied (Fig. 1), allowed us to systematically investigate substrate C assimilation while
102 maintaining identical conditions across samples. We hypothesized that bacterial contributions to
103 the soil C-cycle are governed by microbial life history strategies. We predicted that bacteria
104 could be grouped into ecologically relevant clusters based on their C assimilation dynamics.
105
106 **Results and discussion**

107 *Substrate bioavailability explains carbon mineralization rates*

108 We tracked C mineralization dynamics for each substrate over 48 days by measuring
109 $^{13}CO_2$ production. Peak substrate ^{13}C mineralization rates occurred on different days: day 1 for
110 glucose and amino acids; day 2 for xylose, glycerol, and vanillin; day 3 for lactate; day 7 for
111 oxalate; day 10 for cellulose; and day 14 for palmitic acid (Fig. 2A). Cumulative ^{13}C
112 mineralization varied substantially between substrates, being lowest for vanillin (42% C
113 mineralized to CO_2) and highest for oxalate (88% C mineralized, Fig. 2B). As expected, total C
114 mineralization (^{13}C + ^{12}C) was similar across all treatments (Fig. S1) since all microcosms
115 received the same set of substrates and only the identity of the isotopically labeled substrate
116 varied. These mineralization dynamics were confirmed in an independent experiment with soils
117 from the same site (Fig. S2).

118 Since substrate bioavailability can predict degradation rate in soil [50], we used
119 substrates with differing bioavailability as measured by the octanol-water partition coefficient
120 (Kow). We found a significant negative correlation between Kow, and maximum mineralization
121 rate (R^2 = 0.82, p-value < 1E-3; Fig. S3A) and a significant positive correlation between Kow
122 and the day when maximal rates occurred (R^2 = 0.82, p-value < 1E-3; Fig. S3B). These findings
123 confirm that substrates with low bioavailability, such as cellulose (an insoluble polymer) and
124 palmitic acid (a fatty acid), are degraded slowly, while those with high bioavailability, such as
125 glucose, xylose, amino acids, and lactate are degraded rapidly. Vanillin (an aromatic molecule)
126 had intermediate bioavailability allowing it to be mineralized rapidly, however its
127 hydrophobicity favors adsorption to organic surfaces in soil [51, 52]. Hence, while vanillin in the
128 aqueous phase degrades rapidly, its sorption to organic matter limits microbial access over time.

129 Highly oxidized compounds such as oxalate favor allocation of C to catabolic processes,
130 resulting in greater cumulative mineralization [53, 54].
131
132 *Bacteria active in C-cycling include non-cultivated representatives*
133 The temporal dynamics of microbial C assimilation were assessed by performing MW-
134 HR-SIP for each of the nine ^{13}C-labeled substrates over 48 days. Sampling times were selected
135 based on the ^{13}C mineralization dynamics for each substrate. A total of 12,394 unique bacterial
136 OTUs were observed and 6,613 of these passed independent filtering on the basis of sparsity.
137 From this set, MW-HR-SIP identified 1,286 "incorporators" (*i.e.,* OTUs with significant
138 evidence of ^{13}C incorporation into DNA; Fig. 3; supplemental dataset). We also examined
139 unfractionated DNA (*i.e.,* DNA extracted directly from soil and not subjected to MW-HR-SIP) in
140 order to evaluate overall change in microbial community composition over time. The majority of
141 incorporators were also detected in unfractionated DNA (1,153, or about 90%), through 133
142 incorporators (~10%) were not observed in unfractionated DNA. This result indicates that rare
143 OTUs, not readily detected in 16S rRNA gene surveys, were active participants in soil C-cycling.
144 Density gradient centrifugation fractionates DNA by buoyant density and this technique will
145 often reveal rare taxa not readily observed when sequencing unfractionated soil DNA.
146 Only 13.6% of the incorporators matched known cultivated isolates (*i.e.,* > 97% 16S
147 rRNA gene sequence identity to known isolates), 59.6% had no closely related isolate (*i.e.,* <
148 97% 16S rRNA gene sequence identity), and 26.8% were distantly related to any known isolate
149 (*i.e.,* < 90% 16S rRNA gene sequence identity). C from substrates of low bioavailability (*i.e.,*
150 cellulose, palmitic acid, and vanillin) were incorporated primarily by non-cultivated OTUs (Fig.
151 S4). In contrast, C from substrates of high bioavailability (*i.e.,* glucose, xylose, amino acids,

152 glycerol, oxalate, and lactate) were incorporated primarily by OTUs matching known isolates
153 (Fig. S4). Microbes adapted for growth on low bioavailability substrates are likely to have traits
154 (*e.g.,* slow growth, metabolic dependency, surface attachment) that diminish their tolerance for
155 laboratory growth media and may limit their representation in culture collections [55, 56].
156
157 *Phylogenetic conservation of C assimilation dynamics*
158 The ecophysiology of bacterial OTUs is often inferred from their phylogenetic
159 relatedness [57–60]. We therefore sought to determine if C assimilation activity could be
160 predicted on the basis of phylogeny. We used two methods to test for the phylogenetic
161 conservation of C assimilation dynamics. First, we calculated the distance in realized activity
162 between OTUs (*i.e.,* dissimilarity in ^{13}C assimilation dynamics across all nine substrates).
163 Realized activity was weakly conserved among closely related taxa and this functional distance
164 increased rapidly with phylogenetic distance (Fig. 4A-B). Even when analyzing ^{13}C assimilation
165 dynamics from each substrate independently, phylogeny was poor predictor of realized function
166 (Fig. S5). Second, we used consenTRAIT [59] to measure the phylogenetic depth (*i.e.,* 16S
167 rRNA gene evolutionary distance; τ_D) at which patterns of ^{13}C assimilation were conserved. We
168 found τ_D values ranging from ~0.001 to 0.025 across the nine substrates (Fig. 4C), consistent
169 with τ_D values of carbon substrate utilization measured by Martiny et al. [59]. There was a
170 significant correlation between τ_D and time of assimilation (linear least squares regression; R^2 =
171 0.62, p-value < 1E-7; Fig. 4C). More specifically, phylogenetic depth was highest for vanillin,
172 cellulose, and palmitic acid when assimilated at later time points, though the phylogenetic
173 clustering of bacteria that assimilated C from these substrates was not statistically significant
174 from random across all time points (consenTRAIT; adjusted p-value ≥ 0.05; Fig. 4C). These

175 results suggest that the assimilation of C from low bioavailability substrates requires metabolic
176 capabilities or traits that are more deeply conserved that those capabilities required to assimilate
177 C from high bioavailability substrates.

178 Our results indicate that there is little phylogenetic conservation of *in situ* C assimilation
179 dynamics at taxonomic ranks above the species level (Fig. 4A-B), and that phylogenetic
180 relatedness is therefore a weak predictor of realized bacterial function in soil C-cycling. This
181 result stands in contrast to the observation that bacterial metabolic *potential* (*i.e.,* the presence or
182 absence of genes and pathways) exhibits strong phylogenetic conservation [59]. Our results
183 demonstrate the discrepancy between '*realized function*' as it occurs in soil and '*potential*
184 *function*' encoded in the genome. Realized function is determined by genetic potential (G) and
185 environmental characteristics (E), and G x E interactions exert powerful controls on trait
186 expression and fitness in ecological systems. Furthermore, ecological interactions, such as
187 competition, facilitation, and antagonism likely have profound impacts on the realized function
188 of microbes in soil [27].

189

190 *Patterns of C assimilation delineate bacteria across life history strategies*

191 Since phylogenetic relatedness was a weak predictor of substrate assimilation dynamics
192 in soil, we sought an alternative means to group bacteria into ecologically relevant clusters. We
193 used unsupervised clustering to group incorporators based on their ^{13}C labeling dynamics. This
194 approach generated 28 functional clusters (FC) composed of bacteria that shared similar patterns
195 of C assimilation (Fig. 5A; supplemental dataset). Each FC contained between 15 and 122
196 incorporators and represented 3 to 13 different phyla.

197 To better understand the ecological relevance of these clusters, we evaluated the manner
198 in which 5 properties varied among the 28 FC. These properties were selected as potential
199 indicators of bacterial life history strategies: predicted rRNA operon (*rrn*) copy number, the
200 timepoint ^{13}C-labeling was first observed, the number of substrates from which C was
201 incorporated, the average bioavailability of substrates from which C was incorporated, and the
202 initial relative abundance in the soil community. We used principal component analysis (PCA) to
203 differentiate FC on the basis of all five properties (Fig. 5B). The first principal component (PC1)
204 explained 51% of the variation among FC and was largely defined by bioavailability of the
205 substrates from which C was assimilated, the time of first labeling, estimated *rrn* copy number,
206 and initial relative abundance in the community. Linear regression against PC1 revealed a
207 significant positive relationship with initial relative abundance ($R^2 = 0.66$, p-value < 0.001; Fig.
208 S6) and *rrn* copy number ($R^2 = 0.44$, p-value < 0.001; Fig. S6), and a significant negative
209 relationship to bioavailability of the substrates from which C was assimilated ($R^2 = 0.69$, p-value
210 < 0.001; Fig. S6). We propose that PC1 reflects a continuum of life history strategies ranging
211 from more oligotrophic to more copiotrophic [39]. FC with low PC1 values are more
212 oligotrophic in character having low *rrn* copy number and assimilating C slowly from low
213 bioavailability substrates. FC with high PC1 values are more copiotrophic in character having
214 high *rrn* copy number and exhibiting rapid assimilation of C from high bioavailability substrates.
215 The copiotroph-oligotroph framework was first used to describe the life history strategies
216 of aquatic bacteria. Aquatic oligotrophs thrive at low substrate concentrations where substrate
217 flux across the membrane is low and this imposes selection for high metabolic efficiency [41, 42,
218 62–67]. Aquatic oligotrophic habitats are characterized by substrates that have low concentration
219 at steady state [68]. Under such equilibrium conditions, oligotroph growth rates are governed by

220 substrate affinity as described by Michaelis-Menton kinetics [41]. Soils, however, represent a
221 highly dynamic non-equilibrium system in which substrate availability varies over time in
222 response to nutrient inputs and water availability [69].

223 Soil drying limits diffusion dramatically, resulting in periods of substrate limitation even
224 if nutrients are otherwise abundant in bulk soil, while soil wetting enhances diffusive transport of
225 soluble nutrients. Hence, wetting and drying of soil have major impacts on nutrient availability
226 dynamics. Insoluble substrates, and those substrates adsorbed to surfaces, are unable to cross the
227 cytoplasmic membrane. Growth on these substrates is limited by the diffusion of enzymes and
228 enzyme products between cells and their substrates. As a result, we predict that growth on low
229 bioavailability substrates favors slow growing oligotrophs, because limitations on diffusion and
230 transport should select for metabolic efficiency. Furthermore, diffusive fluxes are favored by
231 intimate contact between organism and substrate. Such close contacts persist in water films that
232 coat soil aggregates, and remain in place as soils dry and diffusion is limited by increasing
233 tortuosity. Hence, we predict that oligotrophic activity persists over a wide range of moisture
234 availability in soils and that such activity is mediated by diverse collections of interacting
235 organisms. In contrast, we predict that growth on soluble substrates favors copiotrophs, because
236 these substrates are ephemeral in nature outside of the rhizosphere, being transiently available in
237 high concentration as a pulsed resource following wetting events. When soils are dry, water-
238 soluble substrates are poorly available due to diffusional limitation. Wetting provides a flush that
239 delivers these substrates into pore water where they are more accessible and where diffusion is
240 less limited because tortuosity is low. The pulsed nature of soluble organic matter in soil pore
241 water will favor rapid growth when nutrients are transiently present in excess, because the

242 benefits of high affinity only matter when nutrients are present at low concentration and the
243 benefits of high efficiency only matter when nutrients are present at steady state.
244 Copiotroph and oligotroph life history strategists should exhibit different growth
245 dynamics with the former exhibiting rapid population growth when nutrients are available and
246 the latter exhibiting slow, less variable growth over time [39]. We examined relative abundance
247 dynamics for all incorporator OTUs to infer growth dynamics and assessed growth dynamics
248 across the proposed copiotroph-oligotroph continuum (*i.e.,* PC1). As sequencing data is
249 compositional [70], we normalized relative abundance values with respect to DNA yield and
250 predicted *rrn* copy number for each sample. Correction for *rrn* copy number was employed to
251 prevent overestimation of the initial growth response from fast growing organisms which had
252 significantly higher *rrn* copy number than slow growing organisms (Fig. 4B, 6A, S6). We note
253 that, while this normalization method reduces compositionality artifacts and improves
254 representation of OTU relative abundance dynamics, it likely misestimates true population sizes
255 by not accounting for differences in genome size nor differential DNA recovery from *Bacteria*,
256 *Archaea*, and *Eukarya*. For the most copiotrophic FC (PC1 > 0.10), normalized relative
257 abundance increased dramatically over time, reaching a maximum at day 3 followed by a rapid
258 decline (Fig. 6). This dynamic is similar to the "boom and bust" cycles typically observed for
259 conditionally rare or copiotrophic bacteria [39, 71, 72]. For the most oligotrophic FC (PC1 < -
260 0.15) the increase in normalized relative abundance was far slower and less dynamic, reaching a
261 maximum at 30 days (Fig. 6). This slow and steady growth is expected for oligotrophic
262 organisms that have low population turnover rates and efficient yet slower biomass production
263 [39]. FC in the middle of the continuum (-0.15 < PC1 < 0.10), demonstrated intermediate growth
264 dynamics and reached a maximum at day 6 (Fig. 6). We observed an initial transient dip in

normalized relative abundance for the latter two groups. While it is possible that these groups experienced mortality upon wetting of soil, it seems likely, given the large increase in the relative abundance of copiotrophic bacteria, that this dip is an artifact of sequencing compositionality not eliminated by normalization.

We further assessed whether the life history strategies defined along PC1 are phylogenetically conserved, and whether they explain variations in predicted phenotypic traits from the ProTRAITS atlas [26]. PC1 explained a small but significant amount of variation in the phylogenetic composition of FC (Unifrac distance; PERMANOVA, $R^2 = 0.092$, p-value = 1E-4; Fig. 5C). However, there was little evidence that life history strategy was conserved at large taxonomic scales (Fig. S7). PC1 explained a small but significant amount of variation in predicted phenotypic traits (PERMANOVA, $R^2 = 0.032$, p-value < 1E-4; Fig. 5D). These findings further demonstrate that associations with cultured representatives have low capacity to predict realized C-cycling function of soil bacteria.

Beyond the copiotroph-oligotroph continuum

While the copiotroph-oligotroph axis (PC1) explained most variation in C assimilation dynamics, additional variation was described by the PC2 axis (Fig. 5B). Most variation in PC2 occurs at the copiotrophic end (PC1 > 0.1) of the copiotroph-oligotroph continuum, while oligotrophic taxa (PC1 < -0.015) exhibit little variation in PC2. We hypothesize that this differentiation of FC along both PC1 and PC2 is explained by Grime's C-S-R life history framework [35].

The C-S-R framework divides organisms into three strategies (competitors, stress tolerators, and ruderals). While this framework was originally designed to describe plant life

288 history strategies, it has recently been applied to microbial systems [73–75]. Ruderal bacteria (R)
289 would be those that have little investment in resource acquisition, being adapted for rapid growth
290 in response to non-equilibrium conditions during nutrient pulses and disturbance. Competitive
291 bacteria (C) can also grow rapidly but are adapted for yield because they allocate more energy to
292 resource acquisition under steady state conditions. Competitors grow with greater efficiency than
293 ruderals but their investments in resource acquisition render them more sensitive to disturbance
294 [75]. In this framework, both ruderals and competitors can be considered copiotrophs because of
295 their tendency to be favored when substrate bioavailability is high [73], but these strategies
296 would manifest differently in their temporal dynamics and sensitivity to non-equilibrium states
297 (*e.g.,* disturbance). The stress tolerator (S) strategy was defined by Grime on the basis of abiotic
298 stress, but we propose that for soil bacteria this category corresponds to tolerance of metabolic
299 stress and that these organisms are adapted for life at low energy flux (*i.e.*, conditions that would
300 result in starvation or dormancy of copiotrophs). In soil, we propose that stress tolerators are
301 therefore synonymous with oligotrophs.
302 While PC1 divides the FC along an oligotroph-copiotroph continuum as described
303 previously, we propose that PC2 divides the FC along a ruderal-competitor continuum. FC with
304 high PC1 and low PC2 values have very high *rrn* copy number, low initial relative abundance,
305 and they tend to assimilate C from a low diversity of highly available substrates. FC with high
306 PC1 and high PC2 values have moderate to high *rrn* copy number, high initial relative
307 abundance, and they tend to assimilate C from diverse substrates likely indicating diverse
308 resource acquisition capabilities (Fig. S8).
309
310 *Life history strategy explains bacterial response to plant residue addition*

311 To further explore the predictive ability of life history strategies to explain microbial C-
312 cycling dynamics *in situ*, we mapped our incorporator OTUs to data from a Whitman et al. 2016
313 [76] study examining plant residue decomposition in agricultural soils. We found a significant
314 positive correlation between an OTU's position on the copiotroph-oligotroph continuum (PC1)
315 and its response to plant litter addition in agricultural fields (Fig. S9). Copiotrophic FC increased
316 significantly in abundance within 12 days of fresh litter addition to soil ($R^2 = 0.304$, p-value =
317 0.002), and these trends persisted over 82 days ($R^2 = 0.211$, p-value = 0.014). The increase and
318 then decline of copiotrophs in response to either fresh litter (Fig S9) or substrate mixture (Fig. 6)
319 suggests a pattern of community succession when a pulse of C is added to soil, a pattern that has
320 been observed and discussed previously [77].
321
322 *C-cycle functionality explains microbial biogeography*
323 We mapped incorporators to global bacterial surveys to determine whether realized C-
324 cycling activity, as defined by FC membership, explained variation in biogeography of soil
325 bacteria. We employed RLQ analysis, a multivariate approach that finds correspondence
326 between organism properties (R) and environmental parameters at various sites (Q; *e.g.,* habitat
327 or soil pH) based on organismal abundance within sites (L) [78, 79]. We mapped incorporator
328 OTUs and their FC membership to two 16S rRNA gene surveys of soil bacterial diversity
329 spanning continental (QIITA study 619) and global scales (QIITA study 928) [80]. FC
330 membership explained significant variation in microbial relative abundance across
331 environmental parameters (Table S1; Fig. S10). At continental scales, FC with high PC1 and
332 high PC2 (competitors) were associated with forest soils, and soils having high organic C and N
333 (DL; Fig. S10A). At global scales, these FC were positively associated with latitude (DL; Fig.

334 S10B), likely as a result of the northern concentration of forest ecosystems and soil organic
335 matter at global scales. The FC that were most strongly associated with tropical and subtropical
336 broadleaf forests were those that most rapidly assimilated C from cellulose (PE; Fig. S10B). The
337 FC that were most strongly associated with temperate grasslands, savannas, and shrubland were
338 generalists that incorporated diverse substrates (DL, PL, and VL; Fig. S10B). FC assigned to the
339 oligotrophic strategy (low PC1) were most closely associated with desert biomes (PL and VL;
340 Fig. S10A). These results show that patterns of microbial C-assimilation can be linked to patterns
341 of microbial biogeography and they suggest that these relationships can be predicted from
342 microbial ecological characteristics derived from life history theory.
343

344 **Conclusions**

345 We conducted a multi-substrate DNA-SIP experiment to measure the *in situ* activities of
346 bacteria in the soil C-cycle. We show that degradation dynamics and patterns of bacterial C
347 assimilation depended on substrate bioavailability. In total, 1286 bacteria were found to
348 incorporate C from the nine substrates assayed, and most of these bacteria were distantly related
349 to cultivated isolates. We found that realized C assimilation dynamics in soil had low
350 phylogenetic conservation among bacteria and were poorly predicted by phylogenetic affinity to
351 cultivated isolates. Instead, variation in C assimilation dynamics were explained by ecological
352 characteristics associated with variation in life history strategies. We also show that shared C
353 assimilation dynamics and ecological characteristics (*i.e.,* functional clusters) predicted
354 community level response when plant litter was added to soil and could explain significant
355 variation in bacterial biogeography. Our results demonstrate that life history strategies are a
356 cogent way to group bacteria by their realized function. SOM is largely derived from the

357 products of anabolic microbial metabolism [14], and therefore microbial assimilation and
358 processing of C over time is a primary determinant of carbon fate in soil. Based on our results,
359 we hypothesize that C fate in soil is not determined primarily by the metabolic pathways that
360 enable its catalysis, but rather it is determined by the life history traits that govern microbial
361 fitness *in situ*. As a result, life history classifications could be useful in predicting the C-cycle
362 activity of microbial communities [18] and SOM dynamics and fate. While more research is
363 necessary to better understand the genetic and ecological underpinnings of life history strategies
364 in soil bacteria, our results add to the growing body of knowledge indicating the importance of
365 life history theory to bacterially mediated terrestrial C-cycling.
366

367 **Materials and methods**

368 *Soil microcosm experiments*

369 Soil microcosms were designed and incubated with ^{13}C-labeled and unlabeled substrates
370 as previously described [47] except that C amendment consisted of nine substrates: cellulose,
371 xylose, glucose, glycerol, vanillin, palmitic acid, amino acid mixture, lactate, and oxalate (SI,
372 Table S2). For most substrates, Kow was determined from reference values, but operational Kow
373 values were estimated for cellulose (which is insoluble) and amino acids (which is a mixture) as
374 described in SI. Each substrate was added at 0.4 mg C g^{-1} soil. Only one of the nine substrates
375 was ^{13}C-labeled in each treatment while the remainder were unlabeled (Fig. 1). Soil was from
376 Penn Yan, New York, USA , with site and collection methods previously described [47, 81] and
377 outlined in SI. ^{13}C and ^{12}C mineralization dynamics were determined based on concentrations of
378 $^{12}CO_2$ and $^{13}CO_2$ in microcosm headspace measured over time as detailed in SI. Soil from

379 microcosms were destructively sampled depending on substrate mineralization dynamics over
380 days 1, 3, 6, 14, 30, and 48 after substrate addition.

381 *DNA extraction and isopycnic centrifugation*

382 DNA extraction and isopycnic centrifugation was conducted as previously described [47]
383 and detailed in SI. In short, for each treatment, size selected DNA (≥ 4 kb) [82] was centrifuged
384 in a CsCl density gradient and 100 µl fractions were collected. An aliquot of DNA taken before
385 isopycnic centrifugation was used for whole microcosm bacterial community sequencing (*i.e.,*
386 unfractionated DNA).

387 *16S rRNA gene amplification and sequencing*

388 We amplified and sequenced the V4 region of the 16S rRNA gene as previously
389 described [83] and detailed in SI using dual indexed primers (515f and 806r) developed by
390 Kozich *et al.* [84]. 16S rRNA amplicon libraries were processed as described previously [47] and
391 detailed in SI. OTUs were clustered at 97% sequence similarity. Raw sequencing reads can be
392 accessed at the NCBI Short Read Archive (accession PRJNA668741).

393 *Identifying incorporators*

394 OTUs that incorporated ^{13}C into their DNA (*i.e.,* incorporators) were identified with
395 MW-HR-SIP [48] using development code for the HTSSIP R package [85]. In short, we used
396 DESeq2 [86] to identify OTUs significantly enriched in the "heavy" gradient fractions of the
397 ^{13}C-labeled treatments compared to the "heavy" gradient fractions in corresponding ^{12}C-control.
398 Incorporators were defined as OTUs with a $\log_2$ fold enrichment greater than 0.25 and a
399 Benjamini-Hochberg adjusted p-value less than 0.1. We used the overlapping BD windows 1.70-
400 1.73, 1.72-1.75, and 1.74-1.77 g/ml, which were shown via simulations to have the highest

401 sensitivity across all tested scenarios while not losing specificity [48]. Independent sparsity
402 filtering was conducted for each BD window to minimize the number of comparisons performed.
403 The taxonomic novelty of incorporators was determined by aligning OTU representative
404 sequences to the Silva all-species living tree project small subunit database version 123,
405 representing all sequenced type strains curated at that time [87]. Alignment was performed using
406 nucleotide BLAST [88] with an expected value cutoff of 1E-20. Incorporators with no hits ≥
407 97% sequence identity were considered to have no closely related isolates, while those with no
408 hits ≥ 90% were considered to have no related isolates. Statistical analyses were conducted in R
409 version 3.1.2 [89].
410 *Analyses of phylogenetic conservation*
411 Fasttree v2.1.9 [90] was used to infer a maximum likelihood phylogeny from the 16S
412 rRNA sequence alignment of representative OTUs. The phylogeny was rooted with *Sulfolobus*
413 *solfataricus* DSM1616 (Genbank accession X90478) as the outgroup. Phylogenetic conservation
414 of realized function was examined both by comparing functional distance with phylogenetic
415 distance and testing for a phylogenetic signal with a modified version of consenTRAIT [59]
416 (https://github.com/nick-youngblut/consenTRAIT).
417 *Analysis of functional clusters (FC)*
418 Incorporators were grouped into FC based on their isotopic labelling response as
419 determined by $\log_2$ fold change in ^{13}C-labeled treatment fractions versus corresponding
420 unlabeled control fractions. Specifically, clustering was performed by: *i*) calculating pairwise
421 Gower distances for each OTU pair, *ii*) hierarchically clustering (UPGMA agglomeration
422 method) based on the resulting distance matrix, *iii*) generating a dendrogram of the hierarchical

423 associations, *iv*) detecting clusters in the dendrogram using the *cutreeHybrid* function in the
424 DynamicTreeCut R package [91].
425 The rRNA operon copy number (*rrn*) of each OTU was predicted as described previously
426 [92]. Briefly, pplacer v1.1 [93] was used to insert OTU representative sequences into a 16S
427 rRNA gene reference phylogeny of bacteria with known *rrn*. The resulting phylogeny was used
428 by guppy v1.1 to predict *rrn* copy numbers of each OTU based on its relatedness to the reference
429 taxa.
430 FC function and trait properties were compared using principal component analysis
431 (PCA) with each property averaged across OTUs within each FC. Functional properties
432 examined were: number of substrates incorporated, initial relative abundance in soil,
433 bioavailability of the substrates incorporated, and time of first labeling, and the trait property
434 used was predicted *rrn* copy number. The two highest principal components were used to
435 classify FC within life history strategies.
436 Changes in OTU relative abundance over time (Fig. 6) were assessed following
437 normalization to minimize compositional data bias. Normalization included two steps:
438 normalizing for DNA yield and normalizing for predicted *rrn* copy number. The extracted ng
439 DNA g^{-1} dry weight soil was quantified with the Quant-iT PicoGreen dsDNA Assay Kit (Thermo
440 Fisher Scientific, Waltham, MA, USA). The relative abundance for each OTU in unfractionated
441 DNA was normalized by first multiplying by sample DNA yield, and then multiplying by a
442 proportion representing the *rrn* copy number of the OTU relative to the summed copy number of
443 the community.
444 *Predicting phenotypic traits of FC*

445 Phenotypic traits were predicted for FC using ProTraits [26]. First, incorporator OTUs
446 were aligned to the microbial 16S rRNA sequence database from the RefSeq Targeted Loci
447 project using nucleotide BLAST [88] with a sequence identity cutoff of 97%. Alignment matches
448 were then mapped to the ProTraits 0.9 precision database [26] based on their unique identifier.
449 Unmapped OTUs were removed from the analysis. Traits were trimmed to just those of interest
450 including primarily metabolisms. Trait scores were averaged across all mapped incorporators
451 within each FC. Trait scores were compared across PC1 from the PCA of FC characteristics by
452 PERMANOVA with averaged phenotypic trait score dissimilarity measured by Bray-Curtis.
453 *Mapping incorporators to independent datasets*
454 Detailed descriptions of the independent datasets and their analysis for this study are
455 found in SI. In short, OTU count tables, representative 16S rRNA gene sequences, and metadata
456 was obtained from the authors for Whitman *et al.* 2016 [76] and downloaded from
457 https://qiita.ucsd.edu/ for QIITA studies 619 (continental dataset) and 928 (global dataset).
458 Incorporators were mapped to external dataset OTUs separately for each study with the mothur
459 alignment tool [94] using the Silva reference alignment as a template. To responses of FC to
460 fresh organic matter addition in Whitman *et al.* 2016 [76] relative abundances of matching OTUs
461 in each field sample were summed within the FC of their mapped incorporators. Then, the
462 enrichment of FC in either PyOM or FOM treatment soils compared to control soils were
463 calculated with DESeq2 [86] with an alternative hypothesis of greater than 1 $\log_2$ fold change
464 enrichment in treatment. To examine the biogeography of FC at continental (QIITA 619) and
465 global (QIITA 928) scales, FC were first grouped for simplicity based on bioavailability of their
466 substrates (D = glucose, xylose, amino acids, glycerol, oxalate, and lactate; V = vanillin; P =
467 cellulose and palmitic acid) and time of labeling (E = first half of timepoints, L = second half of

468 timepoints). Then for each QIITA dataset FC designations (R) of mapped OTUs were used in
469 combination with their OTU count tables (L) and sample metadata (Q) for RLQ and forth corner
470 analyses [79, 95] as detailed in SI.
471

472 **Acknowledgements**
473 We thank Chuck Pepe-Ranney, Ashley Campbell, Marquessa Henry, and Braulio Castillo, Anay
474 Hindupur, and Jillian Waters for their help with experimental design and implementation.
475

476 **Funding**
477 This material is based upon work supported by the Department of Energy Office of Science,
478 Office of Biological & Environmental Research Genomic Science Program under Award
479 Numbers DE-SC0004486 and DE-SC0010558.

References

1. Jobbágy EG, Jackson RB. The vertical distribution of soil organic carbon and its relation to climate and vegetation. *Ecol. Appl.* 2000; 10: 423–436.
2. Brovkin V, Boysen L, Arora VK, Boisier JP, Cadule P, Chini L, *et al.* Effect of anthropogenic land-use and land-cover changes on climate and land carbon storage in CMIP5 projections for the twenty-first century. *J. Clim.* 2013; 26: 6859–6881.
3. Scharlemann JPW, Tanner EVJ, Hiederer R, Kapos V. Global soil carbon: understanding and managing the largest terrestrial carbon pool. *Carbon Manag*. 2014; 5: 81–91.
4. Luo Z, Wang G, Wang E. Global subsoil organic carbon turnover times dominantly controlled by soil properties rather than climate. *Nat. Commun.* 2019; 10: 3688.
5. Bradford MA, Wieder WR, Bonan GB, Fierer N, Raymond PA, Crowther TW. Managing uncertainty in soil carbon feedbacks to climate change. *Nat. Clim. Chang.* 2016; 6: 751–758.
6. Lal R. Soil carbon sequestration impacts on global climate change and food security. *Science* 2004; 304: 1623–1627.
7. Lal R. Soil health and carbon management. *Food Energy Secur. 2016;* 5: 212–222.
8. Reeves DW. The role of soil organic matter in maintaining soil quality in continuous cropping systems. *Soil Tillage Res.* 1997; 43: 131–167.
9. Smith P. Soils as carbon sinks: the global context. *Soil Use Manag.* 2004; 20: 212–218.
10. Heimann M, Reichstein M. Terrestrial ecosystem carbon dynamics and climate feedbacks. *Nature* 2008; 451: 289–292.

11. Todd-Brown KEO, Randerson JT, Hopkins F, Arora V, Hajima T, Jones C, *et al.* Changes in soil organic carbon storage predicted by Earth system models during the 21st century. *Biogeosciences* 2014; 11: 2341–2356.

12. Luo Y, Keenan TF, Smith M. Predictability of the terrestrial carbon cycle. *Glob. Chang. Biol.* 2015; 21: 1737–1751.

13. Wieder WR, Hartman MD, Sulman BN, Wang Y-P, Koven CD, Bonan GB. Carbon cycle confidence and uncertainty: Exploring variation among soil biogeochemical models. *Glob. Chang. Biol.* 2018; 24: 1563–1579.

14. Schimel J, Schaeffer S. Microbial control over carbon cycling in soil. *Front. Microbiol*. 2012; 3: 348.

15. Todd-Brown KEO, Randerson JT, Post MW, Hoffman FM, Tarnocai C, Schuur EAG, S. D. Allison SD. Causes of variation in soil carbon simulations from CMIP5 Earth system models and comparison with observations. *Biogeosciences* 2013; 10: 1717–1736.

16. Wieder WR, Allison SD, Davidson EA, Georgiou K, Hararuk O, He Y, *et al.* Explicitly representing soil microbial processes in Earth system models. *Global Biogeochem. Cycles* 2015; 29: 1782–1800.

17. Wang G, Post WM, Mayes MA. Development of microbial-enzyme-mediated decomposition model parameters through steady-state and dynamic analyses. *Ecol. Appl.* 2013; 23: 255–272.

18. Wieder WR, Grandy AS, Kallenbach CM, Bonan GB. Integrating microbial physiology and physio-chemical principles in soils with the MIcrobial-MIneral Carbon Stabilization (MIMICS) model. *Biogeosciences* 2014; 11: 3899–3917.

523 19. Sulman BN, Phillips RP, Oishi AC, Shevliakova E, Pacala SW. Microbe-driven turnover
524 offsets mineral-mediated storage of soil carbon under elevated CO2. *Nat. Clim. Chang*.
525 2014; 4: 1099–1102.
526 20. Wieder WR, Bonan GB, Allison SD. Global soil carbon projections are improved by
527 modelling microbial processes. *Nat. Clim. Chang.* 2013; 3: 909–912.
528 21. Hug LA, Baker BJ, Anantharaman K, Brown CT, Probst AJ, Castelle CJ, *et al.* A new
529 view of the tree of life. *Nat. Microbiol.* 2016; 1: 16048.
530 22. Lloyd KG, Steen AD, Ladau J, Yin J, Crosby L. Phylogenetically novel uncultured
531 microbial cells dominate earth microbiomes. *mSystems* 2018; 3: e00055-18.
532 23. Steen AD, Crits-Christoph A, Carini P, DeAngelis KM, Fierer N, Lloyd KG, Thrash JC.
533 High proportions of bacteria and archaea across most biomes remain uncultured. *ISME J.*
534 2019; 13: 3126-3130.
535 24. Langille MGI, Zaneveld J, Caporaso JG, McDonald D, Knights D, Reyes JA, *et al.*
536 Predictive functional profiling of microbial communities using 16S rRNA marker gene
537 sequences. *Nat. Biotechnol.* 2013; 31: 814–821.
538 25. Aßhauer KP, Wemheuer B, Daniel R, Meinicke P. Tax4Fun: predicting functional
539 profiles from metagenomic 16S rRNA data. *Bioinformatics* 2015; 31: 2882–2884.
540 26. Brbić M, Piškorec M, Vidulin V, Kriško A, Šmuc T, Supek F. The landscape of
541 microbial phenotypic traits and associated genes. *Nucleic Acids Res.* 2016; 44: 10074–
542 10090.
543 27. Martiny JBH, Jones SE, Lennon JT, Martiny AC. Microbiomes in light of traits: A
544 phylogenetic perspective. *Science* 2015; 350: aac9323.

545 28. Choi J, Yang F, Stepanauskas R, Cardenas E, Garoutte A, Williams R *et al.* Strategies to
546 improve reference databases for soil microbiomes. *ISME J.* 2017; 11: 829–834.
547 29. Fierer N, Leff JW, Adams BJ, Nielsen UN, Bates ST, Lauber CL, *et al.* Cross-biome
548 metagenomic analyses of soil microbial communities and their functional attributes.
549 *Proc. Natl. Acad. Sci. USA* 2012; 109; 21390–21395.
550 30. Alneberg J, Karlsson CMG, Divne AM, Bergin C, Homa F, Lindh MV, *et al.* Genomes
551 from uncultivated prokaryotes: a comparison of metagenome-assembled and single-
552 amplified genomes. *Microbiome* 2018; 6: 173.
553 31. Wohl DL, Arora S, Gladstone JR. Functional redundancy supports biodiversity and
554 ecosystem function in a closed and constant environment. *Ecology* 2004; 85: 1534–1540.
555 32. Evans R, Alessi AM, Bird S, McQueen-Mason SJ, Bruce NC, Brockhurst MA. Defining
556 the functional traits that drive bacterial decomposer community productivity. *ISME J.*
557 2017; 11: 1680–1687.
558 33. Ho A, Di Lonardo DP, Bodelier PLE. Revisiting life strategy concepts in environmental
559 microbial ecology. *FEMS Microbiol. Ecol.* 2017; 93: fix006.
560 34. Stearns SC. Life-history tactics: a review of the ideas. *Q. Rev. Biol.* 1976; 51: 3–47.
561 35. Grime JP. Evidence for the existence of three primary strategies in plants and its
562 relevance to ecological and evolutionary theory. *Am. Nat.* 1977; 111: 1169–1194.
563 36. Stearns SC. Trade-offs in life-history evolution. *Funct. Ecol.* 1989; 3: 259–268.
564 37. Molenaar D, van Berlo R, de Ridder D, Teusink B. Shifts in growth strategies reflect
565 tradeoffs in cellular economics. *Mol. Syst. Biol.* 2009; 5: 323.
566 38. Roller BR, Schmidt TM. The physiology and ecological implications of efficient growth.
567 *ISME J.* 2015; 9: 1481–1487.

568 39. Fierer N, Bradford MA, Jackson RB. Toward an ecological classification of soil bacteria.
569 *Ecology* 2007; 88: 1354–1364.
570 40. Button DK. Kinetics of nutrient-limited transport and microbial growth. *Microbiol. Rev.*
571 1985; 49: 270–297.
572 41. Button DK. Biochemical basis for whole-cell uptake kinetics: specific affinity,
573 oligotrophic capacity, and the meaning of the Michaelis constant. *Appl. Environ.*
574 *Microbiol.* 1991; 57: 2033–2038.
575 42. Button DK. Nutrient-limited microbial growth kinetics: overview and recent advances.
576 *Antonie van Leeuwenhoek* 1993; 63: 225–235.
577 43. Li J, Wang G, Allison SD, Mayes MA, Luo Y. Soil carbon sensitivity to temperature and
578 carbon use efficiency compared across microbial-ecosystem models of varying
579 complexity. *Biogeochemistry* 2014; 119: 67–84.
580 44. Hagerty SB, Allison SD, Schimel JP. Evaluating soil microbial carbon use efficiency
581 explicitly as a function of cellular processes: implications for measurements and models.
582 *Biogeochemistry* 2018; 140: 269–283.
583 45. Dumont MG, Murrell JC. Stable isotope probing — linking microbial identity to
584 function. *Nat. Rev. Microbiol.* 2005; 3: 499–504.
585 46. Hungate BA, Mau RL, Schwartz E, Caporaso JG, Dijkstra P, van Gestel N, *et al.*
586 Quantitative microbial ecology through stable isotope probing. *Appl. Environ. Microbiol.*
587 2015; 81: 7570–7581.
588 47. Pepe-Ranney C, Campbell AN, Koechli CN, Berthrong S, Buckley DH. Unearthing the
589 ecology of soil microorganisms using a high resolution DNA-SIP approach to explore
590 cellulose and xylose metabolism in soil. *Front. Microbiol*. 2016; 7: 703.

591 48. Youngblut, ND, Barnett SE, Buckley DH. SIPSim: A modeling toolkit to predict
592 accuracy and aid design of DNA-SIP experiments. *Front. Microbiol.* 2018; 9: 570.
593 49. Sijm D, Kraaij R, Belfroid A. Bioavailability in soil or sediment: exposure of different
594 organisms and approaches to study it. *Environ. Pollut.* 2000; 108: 113–119.
595 50. Berg B, Hannus K, Popoff T, Theander O. Changes in organic chemical components of
596 needle litter during decomposition. Long-term decomposition in a Scots pine forest.
597 *Botany* 1982; 60: 1310–1319.
598 51. Polubesova T, Chen Y, Navon R, Chefetz B. Interactions of hydrophobic fractions of
599 dissolved organic matter with Fe^{3+}- and Cu^{2+}-Montmorillonite. *Environ. Sci. Technol.*
600 2008; 42: 4797–4803.
601 52. Keiluweit M, Kleber M. Molecular-Level Interactions in soils and sediments: the role of
602 aromatic π-systems. *Environ. Sci. Technol.* 2009; 43: 3421–3429.
603 53. Brant JB, Sulzman EW, Myrold DD. Microbial community utilization of added carbon
604 substrates in response to long-term carbon input manipulation. *Soil. Biol. Biochem*. 2006;
605 38: 2219–2232.
606 54. Manzoni S, Taylor P, Richter A, Porporato A, Ågren GI. Environmental and
607 stoichiometric controls on microbial carbon-use efficiency in soils. *New Phytol.* 2012;
608 196: 79–91.
609 55. Alain K, Querellou J. Cultivating the uncultured: limits, advances and future challenges.
610 *Extremophiles* 2009; 13: 583–594.
611 56. Pham VHT, Kim J. Cultivation of unculturable soil bacteria. *Trends in Biotechnol.* 2012;
612 30: 475–484.

613 57. Lennon JT, Aanderud ZT, Lehmkuhl BK, Schoolmaster DR. Mapping the niche space of
614 soil microorganisms using taxonomy and traits. *Ecology* 2012; 93: 1867–1879.
615 58. Placella SA, Brodie EL, Firestone MK. Rainfall-induced carbon dioxide pulses result
616 from sequential resuscitation of phylogenetically clustered microbial groups. *Proc. Natl.*
617 *Acad. Sci. USA* 2012; 109: 10931–10936.
618 59. Martiny AC, Treseder K, Pusch G. Phylogenetic conservatism of functional traits in
619 microorganisms. *ISME J.* 2013; 7: 830–838.
620 60. Dolan KL, Peña J, Allison SD, Martiny JBH, Phylogenetic conservation of substrate use
621 specialization in leaf litter bacteria. *PLoS One* 2017; 12: e0174472.
622 61. Evans SE, Wallenstein MD. Climate change alters ecological strategies of soil bacteria.
623 *Ecol. Lett.* 2014; 17: 155–164.
624 62. Zobell CE, Grant CW. Bacterial utilization of low concentrations of organic matter. *J.*
625 *Bacteriol.* 1943; 45: 555–564.
626 63. Postgate JR, Hunter JR. The survival of starved bacteria. *Microbiology* 1962; 29: 233–
627 263.
628 64. Jannasch HW. Growth of marine bacteria at limiting concentrations of organic carbon in
629 seawater. *Limnol. Oceanogr.* 1967; 12: 264–271.
630 65. Kuznetsov SI, Dubinina GA, Lapteva NA. Biology of oligotrophic bacteria. *Annu. Rev.*
631 *Microbiol.* 1979; 33: 377–387.
632 66. Akagi Y, Simidu U, Taga N. Growth responses of oligotrophic and heterotrophic marine
633 bacteria in various substrate concentrations, and taxonomic studies on them. *Can. J.*
634 *Microbiol.* 1980; 26: 800–806.

635 67. Button DK. Nutrient uptake by microorganisms according to kinetic parameters from
636 theory as related to cytoarchitecture. *Microbiol. Mol. Biol. Rev.* 1998; 62: 636–645.
637 68. Arnosti C. Microbial extracellular enzymes and the marine carbon cycle. *Ann. Rev. Mar.*
638 *Sci.* 2011; 3: 401–425.
639 69. Sollins P, Homann P, Caldwell BA. Stabilization and destabilization of soil organic
640 matter: mechanisms and controls. *Geoderma* 1996; 74: 65–105.
641 70. Gloor GB, Macklaim JM, Pawlowsky-Glahn V, Egozcue JJ. Microbiome datasets are
642 compositional: and this is not optional. *Front. Microbiol.* 2017; 8: 2224.
643 71. Shade A, Jones SE, Caporaso JG, Handelsman J, Knight R, Fierer N, Gilbert JA.
644 Conditionally rare taxa disproportionately contribute to temporal changes in microbial
645 diversity. *mBio* 2014; 5: e01371-14.
646 72. Balmonte JP, Buckley A, Hoarfrost A, Ghobrial S, Ziervogel K, Teske A, Arnosti C.
647 Community structural differences shape microbial responses to high molecular weight
648 organic matter. *Environ. Microbiol.* 2019; 21: 557–571.
649 73. Prosser JI, Bohannan BJM, Curtis TP, Ellis RJ, Firestone MK, Freckleton RP, *et al.* The
650 role of ecological theory in microbial ecology. *Nat. Rev. Microbiol.* 2007; 5: 384–392.
651 74. Ho A, Kerckhof FM, Luke C, Reim A, Krause S, Boon N, Bodelier PL. Conceptualizing
652 functional traits and ecological characteristics of methane-oxidizing bacteria as life
653 strategies. *Environ. Microbiol. Rep.* 2013; 5: 335–345.
654 75. Fierer N. Embracing the unknown: disentangling the complexities of the soil
655 microbiome. *Nat. Rev. Microbiol.* 2017; 15: 579–590.
656 76. Whitman T, Pepe-Ranney C, Enders A, Koechli C, Campbell A, Buckley DH, Lehmann
657 J. Dynamics of microbial community composition and soil organic carbon mineralization

658 in soil following addition of pyrogenic and fresh organic matter. *ISME J*. 2016; 10: 2918–
659 2930.
660 77. Hu S, van Bruggen AHC. Microbial dynamics associated with multiphasic decomposition
661 of ^{14}C-labeled cellulose in soil. *Microb. Ecol.* 1997; 33: 134–143.
662 78. Dolédec S, Chessel D, ter Braak CJF, Champely S. Matching species traits to
663 environmental variables: a new three-table ordination method. *Environ. Ecol. Stat.* 1996;
664 3: 143–166.
665 79. Dray S, Choler P, Dolédec S, Peres-Neto PR, Thuiller W, Pavoine S, ter Braak CJF.
666 Combining the fourth-corner and the RLQ methods for assessing trait responses to
667 environmental variation. *Ecology* 2014; 95: 14–21.
668 80. Bates ST, Berg-Lyons D, Caporaso JG, Walters WA, Knight R, Fierer N. Examining the
669 global distribution of dominant archaeal populations in soil. *ISME J.* 2011; 5: 908–917.
670 81. Berthrong ST, Buckley DH, Drinkwater LE. Agricultural management and labile carbon
671 additions affect soil microbial community structure and interact with carbon and nitrogen
672 cycling. *Microb. Ecol.* 2013; 66: 158–170.
673 82. Youngblut ND, Buckley DH. Intra-genomic variation in G + C content and its
674 implications for DNA stable isotope probing. *Environ. Microbiol. Rep.* 2014; 6: 767–775.
675 83. Barnett SE, Youngblut ND, Buckley DH. Soil characteristics and land-use drive bacterial
676 community assembly patterns. *FEMS Microbiol. Ecol.* 2019; 96: fiz194.
677 84. Kozich JJ, Westcott SL, Baxter NT, Highlander SK, Schloss PD. Development of a dual-
678 index sequencing strategy and curation pipeline for analyzing amplicon sequence data on
679 the MiSeq Illumina sequencing platform. *Appl. Environ. Microbiol.* 2013; 79: 5112–
680 5120.

681 85. Youngblut ND, Barnett SE, Buckley DH. HTSSIP: An R package for analysis of high
682 throughput sequencing data from nucleic acid stable isotope probing (SIP) experiments.
683 *PLOS ONE* 2018; 13: e0189616.
684 86. Love MI, Huber W, Anders S. Moderated estimation of fold change and dispersion for
685 RNA-seq data with DESeq2. *Genome Biol.* 2014; 15: 550.
686 87. Yarza P, Richter M, Peplies J, Euzeby J, Amann R, Schleifer KH, *et al.* The All-Species
687 Living Tree project: A 16S rRNA-based phylogenetic tree of all sequenced type strains.
688 *Syst. Appl. Microbiol*. 2008; 31: 241–250.
689 88. Altschul SF, Gish W, Miller W, Myers EW, Lipman DJ. Basic local alignment search
690 tool. *J. Mol. Biol.* 1990; 215: 403–410.
691 89. R Core Team. R: A language and environment for statistical computing. 2018.
692 90. Price MN, Dehal PS, Arkin AP. FastTree: Computing large minimum evolution trees
693 with profiles instead of a distance matrix. *Mol. Biol. Evol.* 2009; 26: 1641–1650.
694 91. Langfelder P, Zhang B, Horvath S. Defining clusters from a hierarchical cluster tree: the
695 Dynamic Tree Cut package for R. *Bioinformatics* 2008; 24: 719–720.
696 92. Kembel SW, Wu M, Eisen JA, Green JL. Incorporating 16S gene copy number
697 information improves estimates of microbial diversity and abundance. *PLoS Comput.*
698 *Biol.* 2012; 8: e1002743.
699 93. Matsen FA, Kodner RB, Armbrust EV. pplacer: linear time maximum-likelihood and
700 Bayesian phylogenetic placement of sequences onto a fixed reference tree. *BMC*
701 *Bioinformatics* 2010; 11: 538.
702 94. Schloss PD, Westcott SL, Ryabin T, Hall JR, Hartmann M, Hollister EB, *et al.*
703 Introducing mothur: open-source, platform-independent, community-supported software

704 for describing and comparing microbial communities. *Appl. Environ. Microbiol.* 2009;
705 75: 7537–7541.
706 95. Dray S, Chessel D, Thioulouse J. Co-inertia analysis and the linking of ecological data
707 tables. *Ecology* 2003; 84: 3078–3089.

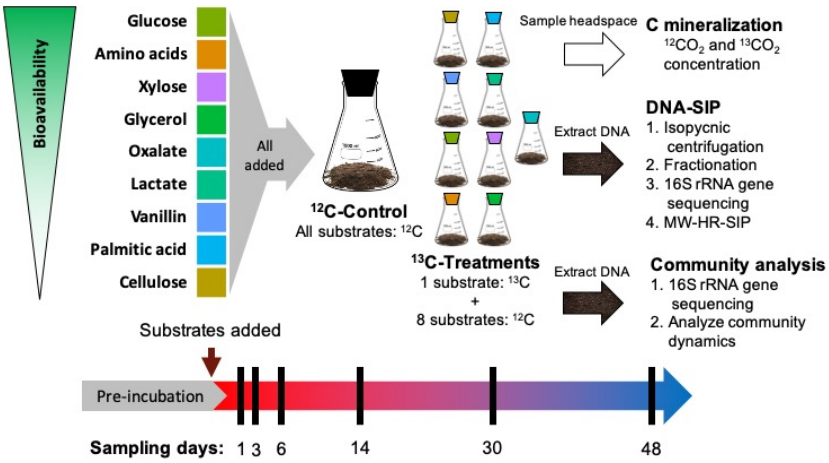

Figure 1: Diagram of the design of the DNA-SIP experiment. This experiment employed soil microcosms, each amended with all nine C substrates (added at 0.4 mg C per gram of soil), only one of which was > 99% ^{13}C-labeled in treatment microcosms. Control microcosms had all nine C substrates added but none were isotopically labeled. Microcosms were destructively sampled at multiple timepoints (black bars) based on mineralization rates from preliminary experiment. Headspace samples were taken every 1-7 days. DNA extracted from microcosm soil was used both for DNA-SIP and whole bacterial community sequencing (unfractionated).

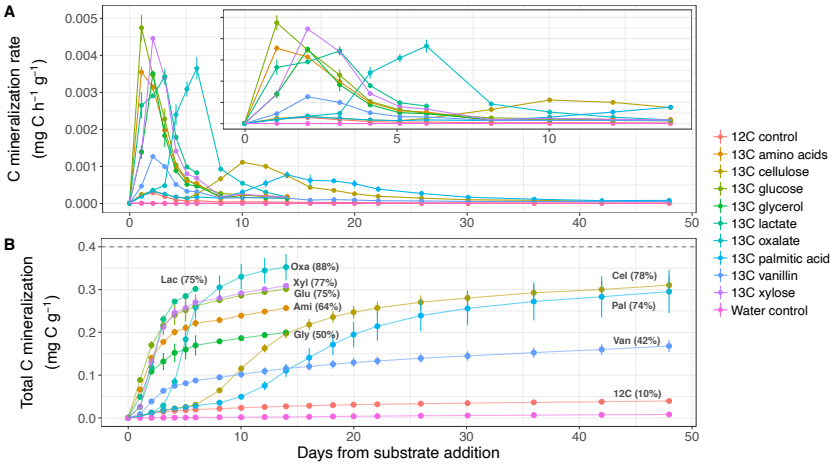

Figure 2: Substrate mineralization dynamics varied based on bioavailability as measured by (A) ^{13}C mineralization rates and (B) cumulative amounts of ^{13}C mineralized. Inset for (A) displays a finer scale representation of the ^{13}C mineralization rates over days 0-14. Error bars represent ± standard deviation among microcosm replicates (n = 3).

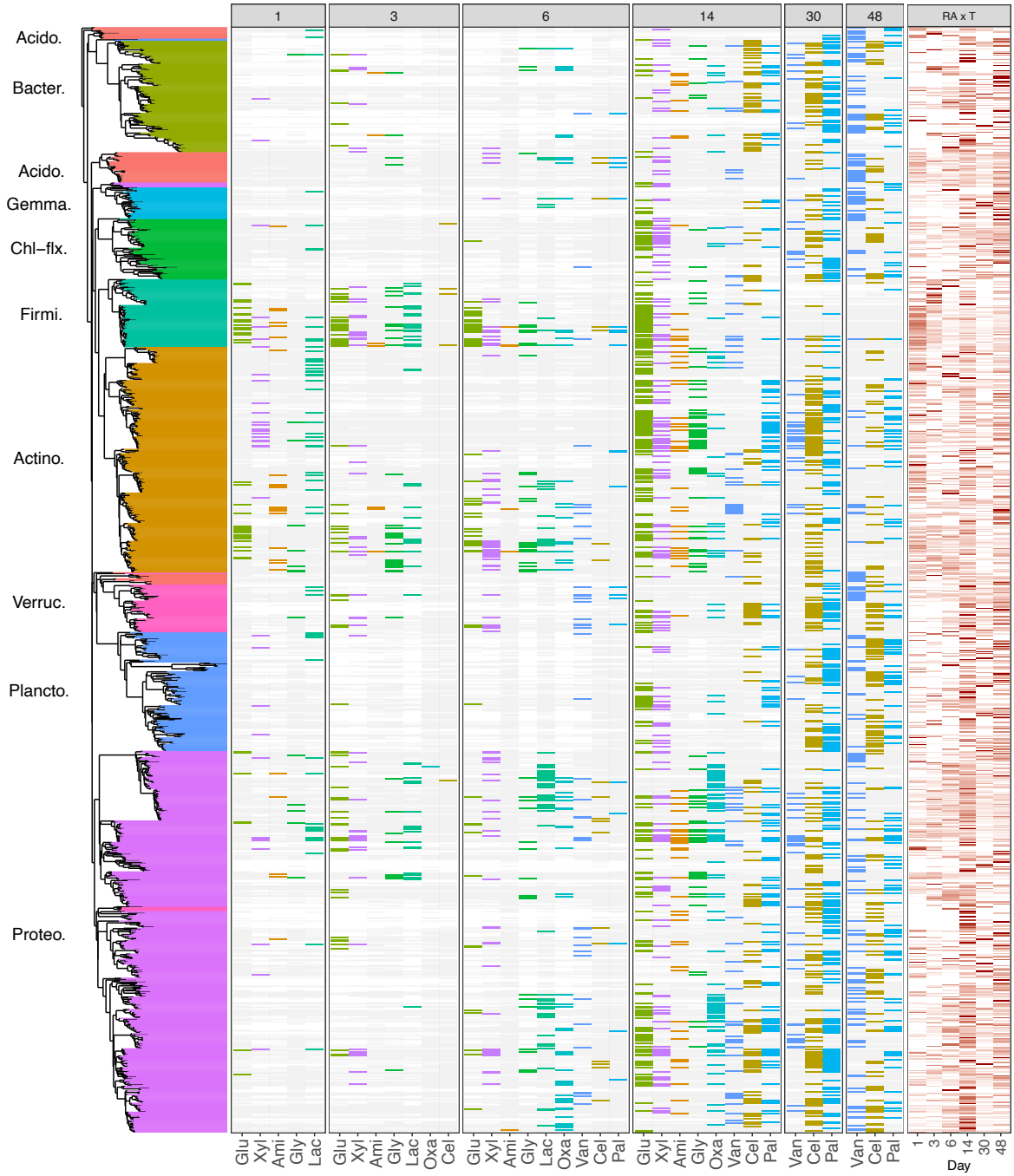

Figure 3: The dynamics of ^{13}C-label incorporation varied by substrate across the 1,286 OTUs that exhibited significant ^{13}C-labelling. OTUs are ordered by their phylogeny with Phyla indicated by different colors. Each vertical block indicates ^{13}C-labelling results for a single day as indicated (days 1, 3, 6, 14, 30, and 48). Each column within a block indicates results for a given ^{13}C-substrate within that day (Glu = glucose, Xly = xylose, Ami = amino acids, Gly =

glycerol, Lac = lactate, Oxa = oxalate, Cel = cellulose, Van = vanillin, Pal = palmitic acid). Rows indicate the ^{13}C-labelling dynamics for each OTU as follows: colored bars indicate ^{13}C-labelling, grey bars indicate OTU detection but no evidence of labeling, white bar indicates the OTU was not detected. The rightmost block (RA x T) shows changes in relative abundance over time for each OTU in unfractionated soil samples with white being 0% and red being 100%. Phylum abbreviations are Acido = *Acidobacteria*, Bacter = *Bacteroidetes*, Gemma = *Gemmatimonadetes*, Chl-flx = *Chloroflexi*, Firmi = *Firmicutes*, Actino = *Actinobacteria*, Verruc = *Verrucomicrobia*, Plancto = *Planctomycetes*, and Proteo = *Proteobacteria*.

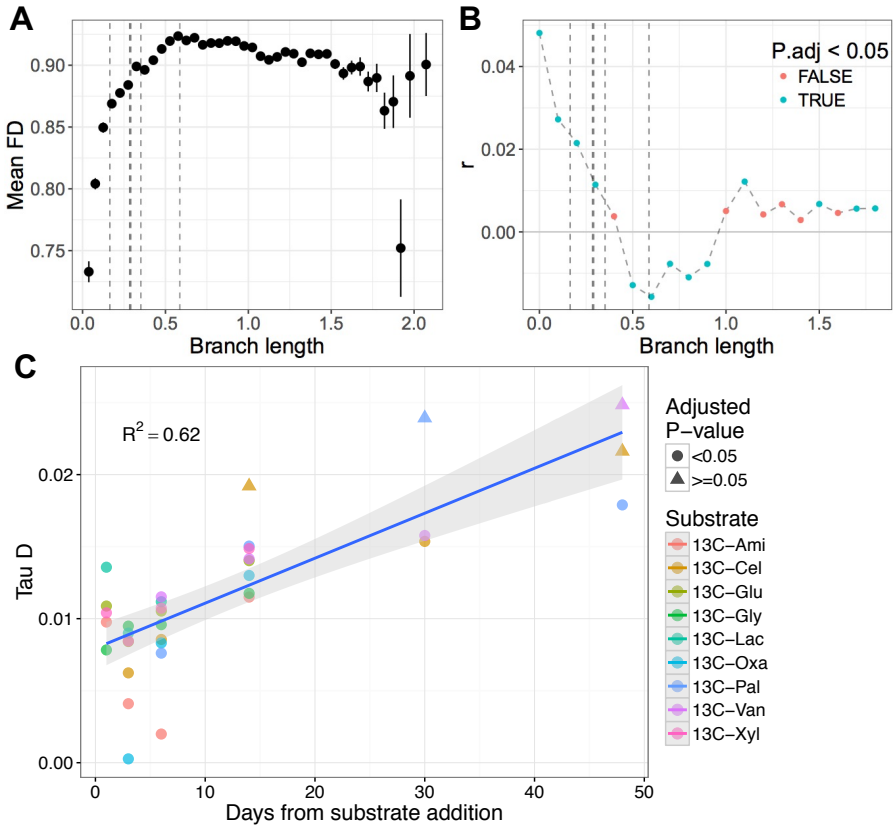

Figure 4: (A) The functional distance (FD) between OTUs, as measured by dissimilarity in substrate incorporation dynamics, increases rapidly in relation to their phylogenetic distance. The vertical dashed lines indicate distance values that correspond to estimates of taxonomic ranks for genus, family, order, class, and phylum (from left to right). (B) Mantel test comparing functional distance and branch length between OTUs with points colored by significance of correlation (Mantel's r). (C) Phylogenetic depth (Tau D) of ^{13}C-labeled with respect to substrate and time derived from consenTRAIT tests. P-values are globally adjusted with the Benjamini-Hochberg correction. The blue line is the linear least squares regression fit ($R^2 = 0.63$, P-value < 1E-7) and the grey ribbon represents the standard error.

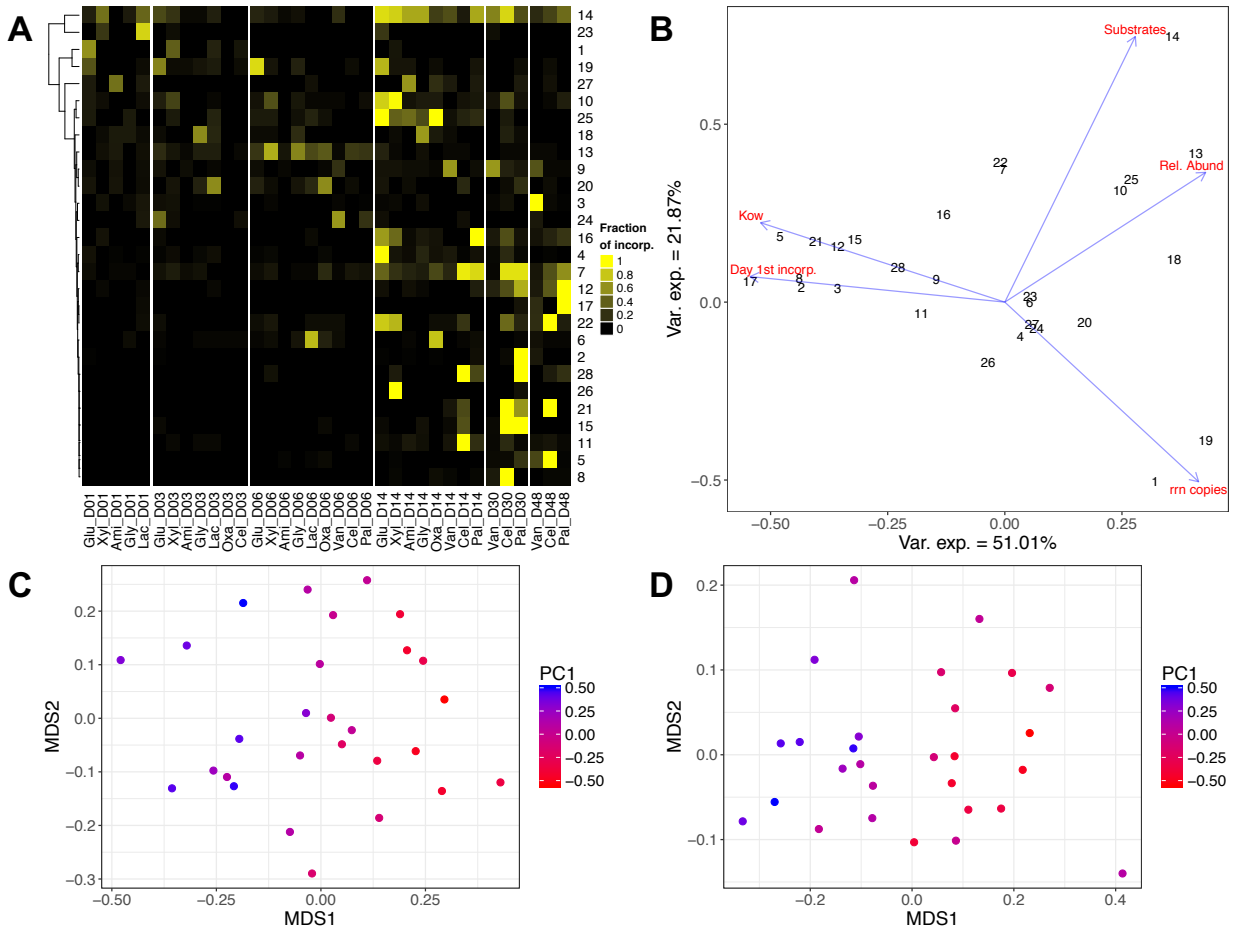

Figure 5: Substrate incorporation dynamics can be used to generate functional clusters (FC) whose collective properties reveal differences in life history strategy. (A) Substrate incorporation dynamics of 28 FC (in rows, sorted by functional similarity) with color indicating the fraction of member OTUs that are ^{13}C-labeled by each substrate on each day (in columns). (B) Principal component analysis (PCA) of FC based on properties associated with life history strategies: number of substrates from which C was assimilated (substrates), the average bioavailability of the substrates from which C was assimilated (Kow), the time of first label incorporation (Day 1st incorp.), the initial relative abundance in soil (Rel. Abund), and rRNA operon copy number (*rrn* copies). Each of the 28 FC are indicated by number. FC variation explained by the first principal component (PC1) segregates FC based upon properties typically associated with the copiotroph (high PC1) to oligotroph (low PC1) continuum. (C) NMDS ordination of FC based on unweighted UniFrac distance indicates that life history strategy (PC1) explains small but significant variation in incorporator phylogeny (PERMANOVA, $R^2 = 0.092$, p-value = 1E-4). (D) NMDS ordination of FC based on phenotypic traits predicted by ProTraits indicates that life history strategy (PC1) also explains small but significant variation in predicted phenotypic traits (PERMANOVA, $R^2 = 0.032$, p-value < 1E-4).

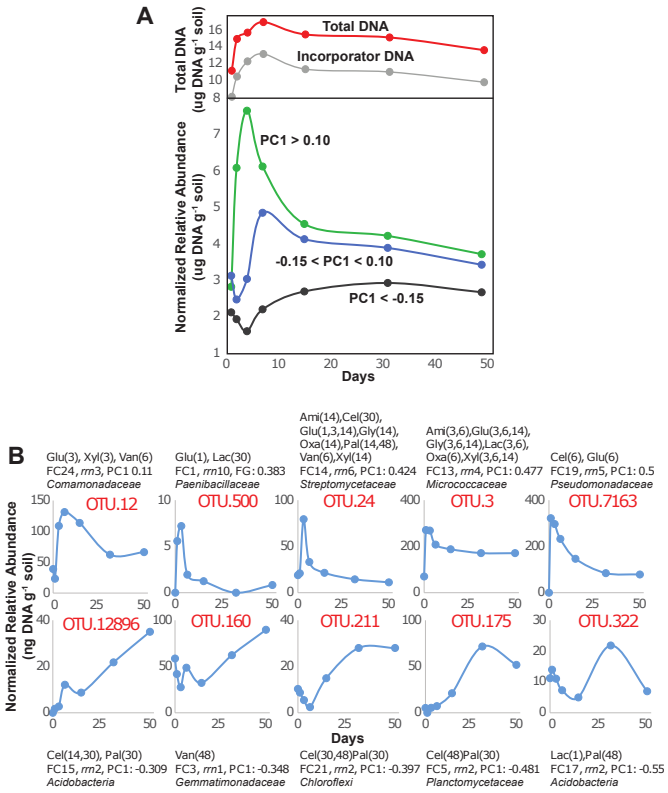

Figure 6: Microbial growth dynamics vary with respect to life history strategy as inferred by position along PC1 (Fig. 5). (A) Total DNA and the summed normalized relative abundance of all ^{13}C-labelled OTUs varied over time, reaching a maximum at day 6 (uppermost panel). The summed normalized relative abundance of all ^{13}C-labelled OTUs classified by their position along PC1 (more copiotrophic, PC1 > 0.10; intermediate, -0.015 < PC1 < 0.10; and more oligotrophic, PC1 < -0.015) varies considerably in soil over time with more copiotrophic taxa exhibiting boom and bust dynamics (lower panel). (B) Normalized relative abundance of individual incorporators in soil over time with more copiotrophic OTUs in the top row and more oligotrophic OTUs in the bottom row. Each OTU is identified along with relevant summary statistics (substrate assimilated and day of labelling, FC membership, *rrn* copy number, PC1 value, phylum affiliation; substrate abbreviations are defined in Fig. 3).